

From short-time diffusive to long-time ballistic dynamics: The unusual center-of-mass motion of quantum bright solitons

Christoph Weiss* and Simon A. Gardiner

Joint Quantum Centre (JQC) Durham-Newcastle, Department of Physics, Durham University, Durham DH1 3LE, United Kingdom

Heinz-Peter Breuer

Physikalisches Institut, Universität Freiburg, Hermann-Herder-Straße 3, D-79104 Freiburg, Germany

(Received 2 April 2015; published 15 June 2015)

Brownian motion is ballistic on short time scales and diffusive on long time scales. Our theoretical investigations indicate that one can observe the exact opposite—an “anomalous diffusion process” where *initially* diffusive motion becomes ballistic on *longer* time scales—in an ultracold atomic system with a size comparable to macromolecules. This system is the center-of-mass motion of a quantum matter-wave bright soliton for which the dominant source of decoherence is *three-particle losses*. Our simulations show that such unusual center-of-mass dynamics should be observable on experimentally accessible time scales.

DOI: [10.1103/PhysRevA.91.063616](https://doi.org/10.1103/PhysRevA.91.063616)

PACS number(s): 03.75.Gg, 05.60.Gg, 03.75.Lm, 67.85.-d

I. INTRODUCTION

Bright solitons—waves that do not change their shape—were discovered in the 19th century in a water canal [1]. Such solitons are good examples of ballistic motion (the distance from the initial position grows linearly with time), as the velocity remains constant. Bright solitons can be experimentally generated from attractively interacting ultracold atomic gases [2–8]; on the mean-field level, via the Gross-Pitaevskii equation (GPE), these matter-wave bright solitons are nonspreading solutions of a nonlinear equation [9–16]. For N ultracold attractively interacting atoms in a (quasi-)one-dimensional wave guide, *quantum* matter-wave solitons [17–24] can be described as a many-particle bound state. This is the ground state [25–27] of an exactly solvable many-particle quantum system, the Lieb-Liniger model [28] with attractive interactions [25]. Already for particle numbers as low as three, these many-particle bound states share many similarities with mean-field matter-wave bright solitons [29].

Diffusive motion (for which the rms fluctuations of the position grow with the square root of time) of both macromolecules and small classical particles often occurs through interactions with the environment: Free Brownian motion [30–36], for example, exhibits the generic short-time-scale ballistic and long-time-scale diffusive behavior. While there are models that, depending on the choice of parameters, behave either diffusively or ballistically [37], in this paper we show the surprising result that the dynamics of the rms fluctuations of the center-of-mass position of quantum bright solitons, under the influence of decoherence via three-particle losses, behaves diffusively on short time scales and ballistically on long time scales.

Deviations from normal diffusion are an ongoing topic of current research. Anomalous diffusion [38] has been observed experimentally in colloidal systems [39,40]; research interest also includes superdiffusive motion [41], which covers a regime in between diffusion and ballistic transport. Diffusive

and ballistic transport, and a surprising transition between the two, are the focus of the current paper.

Diffusive behavior in Bose-Einstein condensates has been observed in the experiment of Dries *et al.* [42], and for matter-wave bright solitons diffusive motion has been predicted in Ref. [43]. In this context it is important to note that, even for a perfect vacuum and when shielded from all external influence, decoherence via three-particle losses will always be present in an atomic Bose-Einstein condensate. The only way to significantly decrease this source of decoherence would be to go to lower densities than is typical for bright solitons as realized experimentally, e.g., in Refs. [2,3]. Thus, we focus on three-particle losses, which is for many parameter regimes the dominant decoherence mechanism (cf. Ref. [44]). For matter-wave bright solitons made of absolute ground-state atoms such as ^7Li [2], there are no two-particle losses [45]; single-particle losses can also be discounted if the vacuum is made to be particularly good (cf. Ref. [46]). It therefore is justified to focus on decoherence via three-particle losses.

The paper is organized as follows: We first introduce the physics involved in opening an initially weak trapping potential in which a bright soliton made from an attractive Bose-Einstein condensate has been prepared (Sec. II). We then introduce the decoherence mechanism which is always present in such a case—atom losses via three-body recombination (Sec. III A), which is modeled via a stochastic approach using piecewise deterministic processes [47] in Sec. III B. Section IV presents the results of our Monte Carlo simulation with the surprising transition from short-time diffusive to long-time ballistic behavior, and the paper ends with a conclusion and outlook (Sec. V).

II. OPENING A WEAK HARMONIC TRAP INTO A QUASI-ONE-DIMENSIONAL WAVE GUIDE

A. Mean-field description: Stationary density profile

When attractively interacting Bose-Einstein condensates are used experimentally to generate bright solitons, the bright soliton is in a (quasi-)one-dimensional wave guide, that is, tight radial confinement and weak axial confinement [2–7]. Important aspects of such bright solitons can be understood by

*christoph.weiss@durham.ac.uk

the one-dimensional (1D) GPE [9]

$$i\hbar \frac{\partial}{\partial t} \varphi = -\frac{\hbar^2}{2m} \frac{\partial^2}{\partial x^2} \varphi + \frac{m\omega^2 x^2}{2} \varphi + g_{1D}(N-1)|\varphi|^2 \varphi, \quad (1)$$

where m is the mass of the particles and ω the angular frequency of the harmonic trap; the interaction $g_{1D} = 2\hbar\omega_{\perp}a$ is set by the s -wave scattering length a and the perpendicular angular trapping frequency, ω_{\perp} [48]. For attractive interactions ($g_{1D} < 0$) and weak harmonic trapping, Eq. (1) has bright-soliton solutions with single-particle densities $n \equiv |\varphi|^2$ [9]:

$$n(x) = \frac{1}{4\xi_N \{\cosh[x/(2\xi_N)]\}^2}, \quad (2)$$

where the soliton length is given by

$$\xi_N \equiv \frac{\hbar^2}{m|g_{1D}|(N-1)}. \quad (3)$$

If the sufficiently weak (the soliton length ξ_N should be small compared to the axial harmonic oscillator length $\sqrt{\hbar/(m\omega)}$ [49]) harmonic trap is then switched off, hardly any atoms are excited [49]. Thus, for bright solitons described on the mean-field (GPE) level, there will be no dynamics observable after opening the trap, whereas we show in the following section (Sec. II B) that the same is not true for quantum bright solitons.

B. Quantum many-body description: Expansion of the center-of-mass wave function

In the absence of a trapping potential in the x direction, the direction of the wave guide, all physically realistic N -particle models have to be translationally invariant in the x direction [using the convention introduced in Eq. (1) as the direction of the wave guide; y and z directions are harmonically trapped]. Thus, the center-of-mass eigenfunctions in the direction of the wave guide are plane waves and the center-of-mass dynamics resembles that of a heavy single particle, with the center-of-mass dynamics described by the Hamiltonian

$$\hat{H} = -\frac{\hbar^2}{2Nm} \frac{\partial^2}{\partial X^2} \quad (4)$$

and the center-of-mass coordinate given by the average of the positions of all N particles,

$$X = \frac{1}{N} \sum_{j=1}^N x_j. \quad (5)$$

The dynamics of the center of mass of an interacting gas in a harmonic potential is independent of the interactions, giving rise to the so-called Kohn mode [50]. Therefore, the initial center-of-mass wave function is independent of both the interactions and the approximate modeling of these interactions.

Thus, the dynamics of the quantum bright soliton in the absence of potentials is due to the center-of-mass wave function of a particle of mass $M = Nm$ [44,51]. As the initial center-of-mass wave function is Gaussian, its time dependence is [52]

$$\Psi(X,t) \propto \left(1 + i \frac{\hbar t}{2M\Delta X_0^2}\right)^{-1/2} \times \exp\left(-\frac{X^2 - i2\Delta X_0^2 M V_0 [X - V_0 t]/\hbar}{4\Delta X_0^2 [1 + i\hbar t/(2M\Delta X_0^2)]}\right), \quad (6)$$

where X is the center-of-mass coordinate (5) and V_0 the initial velocity. This implies an rms width of [52]

$$\Delta X = \Delta X_0 \sqrt{1 + \left(\frac{\hbar t}{2M\Delta X_0^2}\right)^2}. \quad (7)$$

For attractively interacting atoms ($g_{1D} < 0$), the Lieb-Liniger(-McGuire) Hamiltonian [25,28] is a very useful model:

$$\hat{H} = -\sum_{j=1}^N \frac{\hbar^2}{2m} \frac{\partial^2}{\partial x_j^2} + \sum_{j=1}^{N-1} \sum_{n=j+1}^N g_{1D} \delta(x_j - x_n), \quad (8)$$

where x_j denotes the position of particle j . For this model, even the (internal) ground-state wave function is known analytically. Including the center-of-mass momentum K , the corresponding eigenfunctions relevant for our dynamics read (cf. Ref. [27])

$$\Psi(x_1, x_2, \dots, x_N) \propto e^{iKX} \exp\left(-\frac{m|g_{1D}|}{2\hbar^2} \sum_{j<v} |x_j - x_v|\right); \quad (9)$$

the center-of-mass coordinate is given by Eq. (5). If the center-of-mass wave function is a δ function and the particle number is $N \gg 1$, then the single-particle density can be shown [26,27] to be equivalent to the mean-field result (2). Thus, the Lieb-Liniger model is a one-dimensional many-particle quantum model that can be used to justify the approach to treat a quantum bright soliton like a mean-field soliton with additional center-of-mass motion after opening a weak initial trap. In the limit $N \rightarrow \infty$, $g_{1D} \rightarrow 0$ such that $Ng_{1D} = \text{const}$, the initial width of the center-of-mass wave function goes to zero, $\Delta X_0 \propto 1/\sqrt{N}$.¹

C. Single-particle density in the absence of decoherence

Although the center-of-mass wave function (6) spreads according to Eq. (7), a single measurement of the atomic density via scattering light off the soliton (cf. Ref. [2]) will still yield the density profile of the soliton (2), expected both on the mean-field (GPE) level and on the N -particle quantum level for vanishing width of the center-of-mass wave function [26,27]. Taking into account harmonic trapping perpendicular to the x axis, one obtains the density [2]

$$n(x, y, z) = \frac{N}{4\xi_N \{\cosh[x/(2\xi_N)]\}^2} \frac{1}{\lambda_{\perp}^2 \pi} \exp\left(-\frac{y^2 + z^2}{\lambda_{\perp}^2}\right), \quad (10)$$

where $\lambda_{\perp} \equiv \sqrt{\hbar/(m\omega_{\perp})}$ is the perpendicular harmonic oscillator length. In order to experimentally measure the spreading of

¹Only for time scales $\propto \sqrt{N}$ does the width (7) of the center-of-mass wave function become visible when approaching the limit $N \rightarrow \infty$, $g_{1D} \rightarrow 0$ such that $Ng_{1D} = \text{const}$. While such an agreement between GPE and N -particle quantum physics can be expected for some ground states [53], this is not necessarily true for many-particle dynamics [54].

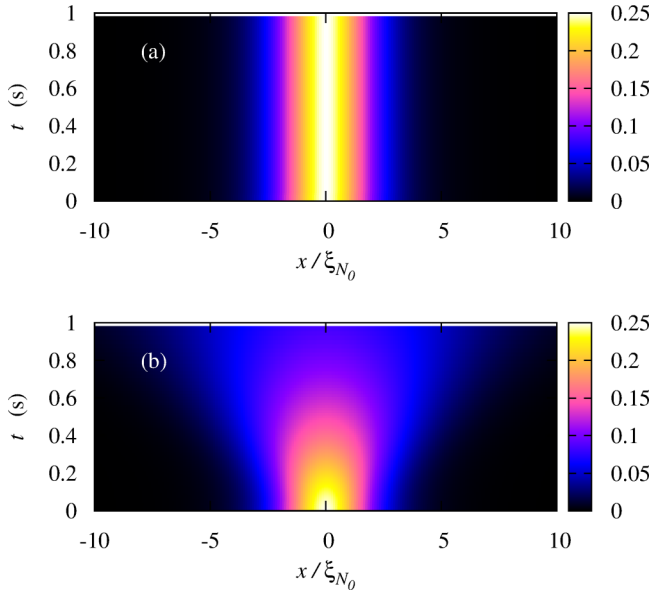


FIG. 1. (Color online) Schematic display of the center-of-mass motion of a bright soliton without decoherence. Shown is the two-dimensional projection of the single-particle density as a function of both time (measured in seconds) and distance from the origin (measured in units of the initial soliton width ξ_{N_0}) for $N = 3000$ Li atoms (using the parameters of Ref. [2]) after opening a weak initial harmonic trap ($\lambda_{\text{HO}} = 10\xi_{N_0}$) at $t = 0$. (a) On the GPE level, the soliton remains stationary; the single-particle density is given by Eq. (2). (b) On the many-particle quantum level, the ballistically expanding center-of-mass wave function smears out the single-particle density.

the center-of-mass density directly, each measurement of the soliton should only record its center-of-mass position when calculating the density from the experimental data. Recording the entire density profile in each measurement yields the single-particle density, which can also be obtained on a more formal level as a sum over the positions \vec{x}_j of all particles $n(\vec{x}) = \sum_{j=1}^N \langle \delta(\vec{x} - \vec{x}_j) \rangle / N$.

Figure 1 shows the influence of the center-of-mass position on the single-particle density of a quantum bright soliton of 3000 Li atoms (as experimentally investigated at high velocities in Ref. [2]). The GPE soliton remains stationary [Fig. 1(a)]; that is, the single-particle density is given by Eq. (2) for all times. Figure 1(b) displays the same situation as Fig. 1(a) but for a quantum bright soliton for which the center-of-mass wave function spreads according to Eq. (7). Thus, for a quantum bright soliton we have a spreading single-particle density, although each single measurement yields the mean-field soliton density [Fig. 1(a)], shifted from the initial position by some distance.

For each single experiment, measuring the center-of-mass density of the many-particle configuration can be done with greater accuracy than the width of the cloud (cf. Ref. [55]). The expansion of the center-of-mass wave function leads to the spreading of the single-particle density; in this paper we consider this spreading in the absence of harmonic trapping potentials. Recent experiments for homogeneous Bose gases can be found in Refs. [56,57].

III. DECOHERENCE VIA THREE-PARTICLE LOSSES

A. Three-particle losses

Three-particle losses can be described by a density-dependent rate equation [45]:

$$\frac{dN}{dt} = -K_3 \int d^3r n^3(x, y, z), \quad (11)$$

where K_3 is determined empirically. Combined with Eq. (10) and using the soliton length (3) this yields [58]

$$\frac{dN}{dt} = -\frac{1}{90\pi^2} K_3 \frac{1}{\xi_{N_0}^2 \lambda_{\perp}^4} N^3 = -\frac{1}{\tau_3} (N-1)^2 N^3, \quad (12)$$

with the N -independent time scale:

$$\tau_3 \equiv \frac{90\pi^2}{K_3} \frac{\hbar^4 \lambda_{\perp}^4}{m^2 g_{\text{1D}}^2}. \quad (13)$$

For this equation to be valid at longer time scales (and not just initially), the single-particle density must remain of the form (10) as the width of the wave function in the x direction increases with decreasing particle number. In the following, we show that this assumption is self-consistent, thus allowing us to treat atom losses as point processes (referring to points in time) within our stochastic approach.

For large N , one may approximate Eq. (12) by $dN/dt \simeq -N^5/\tau_3$, which can be solved to give

$$N(t) \simeq N_0 \left(1 + \frac{t}{\tau_{\text{loss}}} \right)^{-1/4}, \quad (14)$$

where

$$\tau_{\text{loss}} \equiv \frac{\tau_3}{4N_0^4}. \quad (15)$$

For large initial particle numbers N_0 and experimentally relevant time scales Eq. (15) is a good approximation to the full time dependence [which will be shown in Fig. 2(a)].

B. Stochastic modeling of decoherence via three-particle losses

If changes to the number of particles in a soliton happen on slow enough time scales, these changes can be modeled as being adiabatic. The shape of the soliton is protected [44] (cf. Ref. [59]) by an energy gap

$$E_{\text{gap}}(N) \equiv E_0(N-1) - E_0(N) = \frac{mg_{\text{1D}}^2 N(N-1)}{8\hbar^2}, \quad (16)$$

where $E_0(N) = -mg_{\text{1D}}^2 N(N^2-1)/(24\hbar^2)$ is the ground-state energy [25] of a system of N 1D point bosons of mass m interacting via attractive δ interactions, described by the Lieb-Liniger Hamiltonian (8).

The energy-time uncertainty yields a characteristic time scale (cf. Ref. [60]) via $E_{\text{gap}}(N)\tau_{\text{soliton}}(N) \propto \hbar$, where

$$\tau_{\text{soliton}}(N) = \frac{\hbar^3}{mg_{\text{1D}}^2 (N-1)^2}. \quad (17)$$

Changes in particle numbers should happen on time scales longer than this time for the process to be adiabatic, and for our approach of treating particle losses as an adiabatic process to be valid. So far, three-particle losses in experiments have not been observed to destroy solitons on short time scales [2].

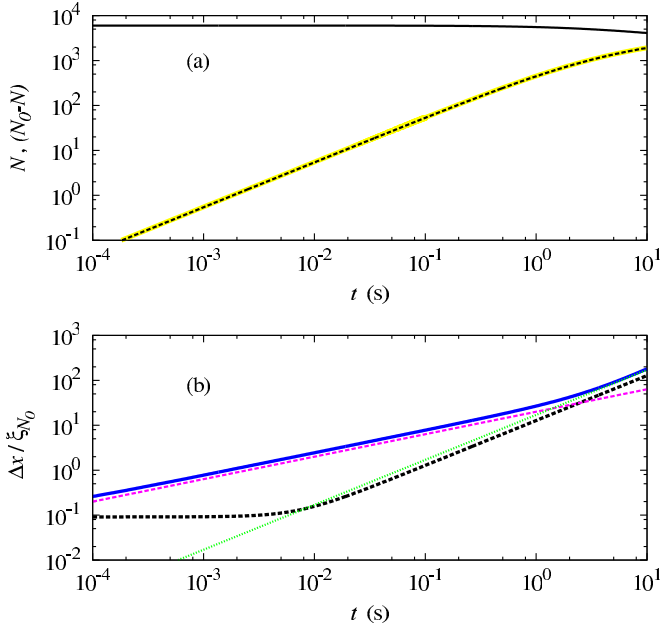


FIG. 2. (Color online) Influence of decoherence via three-particle losses on particle number and rms width of the single-particle density using the parameters described in footnote 2. (a) Number of particles, $N(t)$, obtained numerically as a function of time (solid black line) with $N(0) = 6000$. For $6000 - N(t)$ as a function of time, the numerical curve (black dashed line) lies on top of the analytic curve [yellow (light gray), Eq. (14)]. (b) As soon as particle losses [modeled via the piecewise deterministic processes described in Sec. III B using Eqs. (19) and (28)] become important, the rms width of the single-particle density of a bright soliton [blue (black) solid line] grows like the square root of time [cf. dashed magenta (dark gray) line] before becoming ballistic at larger times [$\propto t$, green (light gray) line], approaching the width of the center-of-mass wave function without decoherence (black dashed line) for larger times.

We can thus model the particle losses as taking place on time scales longer than the soliton time if the soliton time is smaller than the time scale $t_1 \simeq \tau_3/N^5$ on which a single particle is lost, that is,

$$\frac{\tau_3}{N^5 \tau_{\text{soliton}}(N)} > 1. \quad (18)$$

With $N_0 = 6000$ and the experimental parameters of Ref. [2],²

$$\frac{\tau_3}{\tau_{\text{soliton}}(N_0)} \approx 2 \times 10^{20}. \quad (19)$$

Inequality (18) is fulfilled for the parameters of Ref. [2] if $N \gtrsim 6000$. We can furthermore model the three-particle losses as taking place instantaneously for our stochastic implementation [62–64] of particle losses.

²The set of parameters is used as an example to show that experimentally realistic time scales use the values given in Ref. [2] for the s -wave scattering length $a = -0.21 \times 10^{-9}$ m, $f_{\perp} = 710$ Hz where $\omega_{\perp} = 2\pi f_{\perp}$. For this s -wave scattering length we furthermore divide the calculated value [61] for the thermal K_3 of 3.6×10^{-41} m⁶/s by the factor $3! = 6$ for Bose-Einstein condensates (and thus also bright solitons).

For a Schrödinger cat state [65], a quantum superposition of two “macroscopically” occupied single-particle modes, $|\psi_{\text{NOON}}\rangle \propto |1\rangle^{\otimes N} + |2\rangle^{\otimes N}$,³ losing three particles leads to a localization in one of the two modes, $|1\rangle^{\otimes(N-3)}$ or $|2\rangle^{\otimes(N-3)}$. Quantum bright solitons are in a spatial quantum superposition given by their center-of-mass wave function; if the center-of-mass wave function is a δ function, the wave function can be approximated by a Hartree-product state consisting of occupying the mean-field (GPE) wave function N times [27]. We thus model the collapse of the wave function into one of these modes as a starting point to describe the influence of decoherence via three-particle losses on the center-of-mass motion of quantum bright solitons.

We can use the Schrödinger equation for a single particle of mass Nm with Hamiltonian $\hat{H} = -[\hbar^2/(2Nm)]\partial^2/\partial X^2$ to describe the quantum-mechanical motion of the center of mass X of a quantum bright soliton in the absence of decoherence events [44]. Note that the particle number N remains constant between loss events.

For the internal degrees of freedom, we can use a Hartree-product state [9] of bright-soliton solutions of the GPE (1),

$$\psi_{V_0, N}(\underline{x}_N) = \left\{ \frac{e^{iNmV_0x/\hbar - i(\mu - Nm v^2/2)t/\hbar}}{2\sqrt{\xi_N} \cosh[(x - X_0 + V_0t)/(2\xi_N)]} \right\}^{\otimes N} \quad (20)$$

with $\mu = g_{1D}(N-1)/(8\xi_N)$ and $\underline{x}_N = \{x_1, x_2, \dots, x_N\}$. After the three-particle loss, the internal degrees of freedom are described by the wave function given by Eq. (20) with N replaced by $N-3$. As we describe below, both the position and the velocity (via the center-of-mass density) as well as the point of time for this decoherence [via Eq. (12)] are determined via random numbers in a Monte Carlo simulation. A characteristic size for the new center-of-mass wave function is the root-mean-square width of the soliton (cf. Appendix),

$$\Delta x_{\text{soliton}} = \frac{\pi \xi_{N-3}}{\sqrt{3}}. \quad (21)$$

In order to describe the stochastic process, we introduce an approach via a classical master equation. While at first glance this approach may seem to be impossible, as between loss events we have a purely quantum-mechanical expansion of the center-of-mass wave function, the fact that our system can indeed be described by a classical model is justified below. Within our model the stochastic variables are given by the center-of-mass coordinate X , the corresponding velocity V , and the particle number N . Introducing the time-dependent probability distribution $P(X, V, N, t)$ the stochastic process is defined by the master equation

$$\begin{aligned} & \frac{\partial}{\partial t} P(X, V, N, t) \\ &= -V \frac{\partial}{\partial X} P(X, V, N, t) \\ &+ \int dX' \int dV' [W_{N+3}(X, V|X', V') P(X', V', N+3, t) \\ &- W_N(X', V'|X, V) P(X, V, N, t)]. \end{aligned} \quad (22)$$

³The tensor product power notation $|1\rangle^{\otimes N}$ describes N particles occupying the same single-particle mode $|1\rangle$.

The first term on the right-hand side describes the constant drift of X with velocity V while the second term represents the instantaneous random jumps induced by three-particle losses. The process (X, V, N) is thus a piecewise deterministic process [47] with transition rates

$$W_N(X', V' | X, V) = \Gamma(N) \sqrt{\frac{1}{2\pi\sigma_X^2(N)}} \exp\left(-\frac{(X - X')^2}{2\sigma_X^2(N)}\right) \times \sqrt{\frac{1}{2\pi\sigma_V^2(N)}} \exp\left(-\frac{(V - V')^2}{2\sigma_V^2(N)}\right), \quad (23)$$

where $\sigma_X(N)$ is given by Eq. (21), and

$$\sigma_V(N) = \hbar/[2m(N - 3)\sigma_X(N)].$$

The total transition rate takes the form

$$\Gamma(N) \equiv \int dX' \int dV' W_N(X', V' | X, V) = \frac{(N - 1)^2 N^3}{3\tau_3}, \quad (24)$$

where we have added a factor of 1/3 as three particles are lost each time. We thus have an exponential waiting time distribution

$$F(N, t) = 1 - \exp[-\Gamma(N)t]. \quad (25)$$

To summarize, for the stochastic simulation of decoherence via three-particle losses [64], the ingredients are as follows:

(1) The random variables are

$$N, X_0, V_0. \quad (26)$$

(2) Random numbers for the Monte Carlo process determine

(a) The time of the next decoherence event via Eq. (12) by choosing an exponential distribution of loss times (25), where the factor 1/3 introduced in Eq. (24) is necessary because *three* particles are lost in each step: $N \rightarrow N - 3$;

(b) The center-of-mass position X_0 of the new wave function via the center-of-mass density in real space; and

(c) The center-of-mass velocity V_0 of the new wave function via the center-of-mass density in momentum space.

(3) The center-of-mass wave function corresponding to the product state (20) is chosen to be a Gaussian

$$\psi_{\text{c.m.}} = \exp\left[-\frac{(X - X_0)^2}{2b^2} + i\frac{(N - 3)mV_0}{\hbar}X\right] \quad (27)$$

with a root-mean-square width $\sigma_X(N) = b/\sqrt{2}$ given by Eq. (21):

$$\sigma_X(N) = \frac{\pi\xi_{N-3}}{\sqrt{3}}. \quad (28)$$

In between loss events, the quantum dynamics is known analytically [Eq. (6)]; rather than solving the Schrödinger equation it is possible to do this in a more classical approach:

The truncated Wigner approximation⁴ for the center of mass, which has been used in Ref. [23] to qualitatively mimic quantum behavior on the mean-field level by introducing classical noise mimicking the quantum uncertainties in both position and momentum, is particularly useful here. Both the mean position and the variance calculated via the truncated Wigner approximation (TWA) for the center of mass are identical to the quantum-mechanical result. In order to make both results identical, Gaussian noise has to be added independently to both position $X_0 \rightarrow X = X_0 + \delta X_0$ and velocity $V_0 \rightarrow V = V_0 + \delta V_0$ with $\langle \delta X_0 \rangle = 0$ and $\langle \delta V_0 \rangle = 0$ and root-mean-square fluctuations $\sigma_X(N)$ given by Eq. (28) and by the minimal uncertainty relation

$$\sigma_V(N) = \frac{\hbar}{2(N - 3)m\sigma_X(N)} \quad (29)$$

for the velocity.

The mean position $\overline{x(t)} = \overline{X_0 + V_0 t}$ is thus identical to the quantum-mechanical result; the root-mean-square fluctuations $\Delta x = \sqrt{(\Delta X_0)^2 + (\Delta V_0)^2 t^2}$ coincide with the quantum-mechanical equation (7). Thus, in the absence of both the trap in the axial direction and the scattering processes investigated in Ref. [23], the TWA for the center of mass gives exact results for both the position of the center of mass and the root-mean-square fluctuations of the center of mass for a quantum bright soliton.

IV. RESULTS

Figure 2 shows the influence of decoherence via three-particle losses on the center-of-mass displacement of quantum bright solitons made out of Li atoms for parameters taken from the experiment in Ref. [2] (see footnote 2). Three-particle losses, which could only be prevented by considerably reducing the density of a bright soliton to values much lower than used in experiments such as Ref. [2], and are thus a decoherence mechanism intrinsic to quantum bright solitons, lead to a transition from short-time diffusive to long-time ballistic behavior [Fig. 2(b)]. The numerical simulations were done by using the piecewise deterministic processes [47] described in Sec. III B, a well-established tool to model decoherence [62–64].

Figure 3 shows that the transition from short-time diffusive to long-time ballistic behavior is not dependent on a particular choice of parameters. While details of the curves can look different for different parameters, the transition from short-term diffusive to long-time ballistic behavior is visible in particular after rescaling the time axis with the characteristic time scale given by the atom losses [Eq. (14)], thus using the scaling for which all curves $N(t)/N_0$ would lie on top of each other. Within this scaling, all curves follow the same $\sqrt{t}/\tau_{\text{loss}}$ scaling for *early* scaled times, and they each start deviating off at *different* times.

⁴The truncated Wigner approximation [66] describes quantum systems by averaging over realizations of an appropriate classical field equation (in this case, the GPE) with initial noise appropriate to either finite [67] or zero temperatures [13].

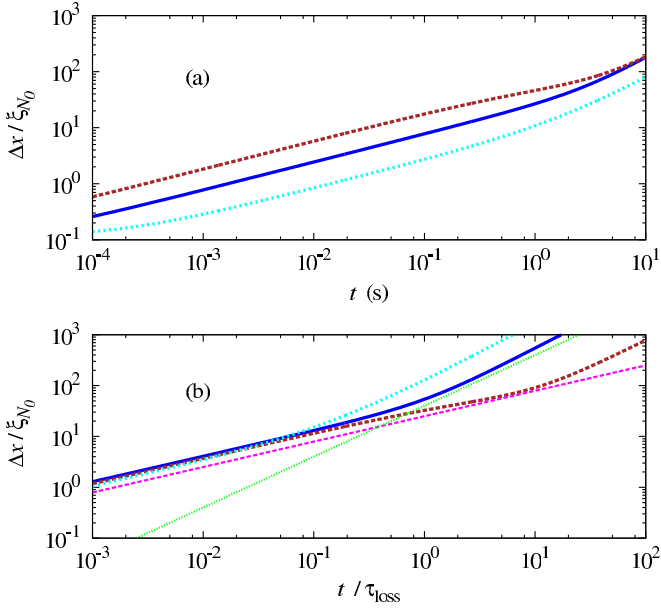


FIG. 3. (Color online) (a) Root-mean-square (rms) width of center-of-mass displacement as a function of time. (a) The data shown are for blue (black) solid line, $N_0 = 6000$, $\tau_3/\tau_{\text{soliton}} = 2 \times 10^{20}$; light blue (light gray) dashed line, $N_0 = 4000$, $\tau_3/\tau_{\text{soliton}} = 1 \times 10^{20}$; brown (black) dashed line, $N_0 = 5000$, $\tau_3/\tau_{\text{soliton}} = 1 \times 10^{19}$. (b) Same data sets as in the previous panel but with a time axis rescaled with the characteristic time from Eq. (15). Both the magenta (dark gray) straight line, $\propto \sqrt{t}$, and the green (light gray) straight line, $\propto t$, were added as guides to the eye.

This scaling leads to an intuitive explanation of the transition from short-time diffusive to long-time ballistic motion. While the atom losses continue in the regime of ballistic motion [as can be seen by comparing Figs. 2(a) and 2(b)], τ_{loss} is the time scale on which $N(t)$ starts to forget its initial number of particles. In addition, the center-of-mass motion also picks up pace for longer time scales. As the GPE becomes valid in the limit $N \rightarrow \infty$, $g_{1D} \rightarrow 0$ such that the product Ng_{1D} remains constant [68], it cannot model an expanding center-of-mass wave function. Thus, the transition from short-time ballistic to long-time diffusive behavior cannot be modeled by simply using standard GPE-theory.

V. CONCLUSION AND OUTLOOK

To conclude, we have introduced a physically motivated model for the motion of quantum bright solitons which displays short-time diffusive and long-time ballistic behavior, contrary to the usual short-time ballistic and long-time diffusive behavior observed, for example, in Brownian motion [34]. Bright solitons are investigated experimentally in various groups worldwide. As the ballistic expansion for large times is $\propto t/(Nm)$ [Eq. (7)], the solitons made of thousands of Li atoms [2] are more suitable to observe this motion of the center of mass than solitons made of thousands of the more than ten times heavier Rb atoms [5]. For the ground-state atoms of Li used, for example, in the ground-breaking experiments in Refs. [2,3] there are no two-body losses [45]; single-particle losses can also be discounted if the vacuum is made to be particularly good (cf. Ref. [46]). Our approach to focus on

decoherence via three-particle losses to model matter-wave bright solitons in attractive Li-Bose-Einstein condensates thus is justified.

The present idea to modify the quantum-mechanical motion by stochastic terms in order to describe instantaneous changes of the wave function to smaller wave packets has formal similarities with stochastic collapse models [69]. However, within our model these random changes describe the decoherence of the center-of-mass wave function which is induced by three-particle losses; a decoherence mechanism which cannot be avoided by, e.g., choosing a perfect vacuum: as long as the density is finite (which always is the case for bright solitons), three-particle losses will occur as a dominant decoherence mechanism. It is the decrease of the particle number that leads to fewer particle losses and, hence, to the observed transition from diffusive to ballistic motion. This motion is an effect distinct from both classical [38] and quantum walks (cf. Refs. [70,71]) as well as anomalous diffusion [38–40]. As for the classical random walk, our model localizes after each step, but between steps the motion is given by free expansion of the center-of-mass wave function which depends on the (decreasing) number of particles.

This unusual behavior of the center-of-mass motion can be observed for experimentally realistic parameters; both time scales and length scales are accessible experimentally. The data presented in this paper are available [72].

ACKNOWLEDGMENTS

We thank S. L. Cornish, S. A. Hopkins, and L. Khaykovich for discussions. C.W. thanks the Institute of Physics, University of Freiburg, for its hospitality. We thank the Engineering and Physical Sciences Research Council (UK) (Grant No. EP/L010844/1, C.W. and S.A.G.) for funding.

APPENDIX: SIZE OF CENTER-OF-MASS WAVE FUNCTION AFTER COLLAPSE

The focus of this paper was to present a physically motivated model which displays a transition from short-time diffusive to long-time ballistic behavior. Time scales can easily be changed by, e.g., choosing a trapping geometry different

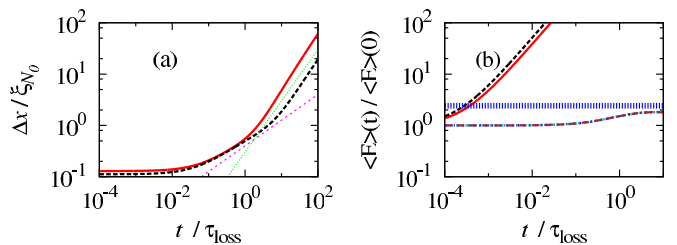


FIG. 4. (Color online) Root-mean-square (rms) width of center-of-mass displacement as a function of time for a model differing from the choice in the main part of the paper (Figs. 2 and 3). Solid red (black) curve, $N_0 = 3000$, $\tau_3/\tau_{\text{soliton}} = 2 \times 10^{15}$; black dashed curve, $N_0 = 4000$, $\tau_3/\tau_{\text{soliton}} = 2 \times 10^{15}$. Dashed magenta (dark gray) line $\propto \sqrt{t}$; green (light gray) line $\propto t$. (b) The kinetic energy as a function of time grows considerably for the two curves of (a) whereas it stays below the line corresponding to $(\langle E \rangle(t) + \Delta E(0))/\langle E \rangle(0)$ [thick blue (black) dashed horizontal line] for the curves of Fig. 3.

from the parameters used in Ref. [2]. The focus currently is on a macroscopic theory; for future microscopic theories some details like the center-of-mass wave function after a decoherence event via the physically dominating decoherence mechanism, a three-particle loss event, might differ from the value chosen here. In order to show that the transition from diffusive to ballistic behavior would still be observable for other choices of the width of the center-of-mass wave function, Fig. 4 displays the behavior for

$$\Delta X_{\text{c.m.}} = \frac{\pi \xi_{N-3}}{\sqrt{3(N-3)}}. \quad (\text{A1})$$

This corresponds to the idealized case that the wave function collapses to a single product state (20); the root-mean-square

width of the new center-of-mass wave function of the soliton consisting of $N - 3$ particles is given by the prediction of the central limit theorem (cf. Ref. [60]).

Figure 4 shows, that as for the choice in the main part of the paper, for Eq. (A1) the combined effect of the rate of particle losses decreasing and becoming more independent of $N(t = 0)$ [cf. Eq. (14)] and the center-of-mass motion covering greater distances leads again to a transition from short-time diffusive to long-time ballistic behavior. However, contrary to the case discussed in the main part of the paper, the kinetic energy is considerably increased during the motion. While the open system discussed in this paper could include such a mechanism, unless experimental results should oblige one to introduce such a mechanism, the model presented in the main part of the paper is the more physical choice.

-
- [1] J. S. Russell, in *Report of the Fourteenth Meeting of the British Association for the Advancement of Science* (John Murray, London, 1845), pp. 311–390.
- [2] L. Khaykovich, F. Schreck, G. Ferrari, T. Bourdel, J. Cubizolles, L. D. Carr, Y. Castin, and C. Salomon, *Science* **296**, 1290 (2002).
- [3] K. E. Strecker, G. B. Partridge, A. G. Truscott, and R. G. Hulet, *Nature (London)* **417**, 150 (2002).
- [4] S. L. Cornish, S. T. Thompson, and C. E. Wieman, *Phys. Rev. Lett.* **96**, 170401 (2006).
- [5] A. L. Marchant, T. P. Billam, T. P. Wiles, M. M. H. Yu, S. A. Gardiner, and S. L. Cornish, *Nat. Commun.* **4**, 1865 (2013).
- [6] P. Medley, M. A. Minar, N. C. Cizek, D. Berryrieser, and M. A. Kasevich, *Phys. Rev. Lett.* **112**, 060401 (2014).
- [7] G. D. McDonald, C. C. N. Kuhn, K. S. Hardman, S. Bennetts, P. J. Everitt, P. A. Altin, J. E. Debs, J. D. Close, and N. P. Robins, *Phys. Rev. Lett.* **113**, 013002 (2014).
- [8] J. H. V. Nguyen, P. Dyke, D. Luo, B. A. Malomed, and R. G. Hulet, *Nat. Phys.* **10**, 918 (2014).
- [9] C. J. Pethick and H. Smith, *Bose-Einstein Condensation in Dilute Gases* (Cambridge University Press, Cambridge, UK, 2008).
- [10] B. B. Baizakov, V. V. Konotop, and M. Salerno, *J. Phys. B* **35**, 5105 (2002).
- [11] U. Al Khawaja, H. T. C. Stoof, R. G. Hulet, K. E. Strecker, and G. B. Partridge, *Phys. Rev. Lett.* **89**, 200404 (2002).
- [12] W. Hai, C. Lee, and G. Chong, *Phys. Rev. A* **70**, 053621 (2004).
- [13] A. D. Martin and J. Ruostekoski, *New J. Phys.* **14**, 043040 (2012).
- [14] J. L. Helm, T. P. Billam, and S. A. Gardiner, *Phys. Rev. A* **85**, 053621 (2012).
- [15] J. Cuevas, P. G. Kevrekidis, B. A. Malomed, P. Dyke, and R. G. Hulet, *New J. Phys.* **15**, 063006 (2013).
- [16] J. Polo and V. Ahufinger, *Phys. Rev. A* **88**, 053628 (2013).
- [17] Y. Lai and H. A. Haus, *Phys. Rev. A* **40**, 854 (1989).
- [18] P. D. Drummond, R. M. Shelby, S. R. Friberg, and Y. Yamamoto, *Nature (London)* **365**, 307 (1993).
- [19] L. D. Carr and J. Brand, *Phys. Rev. Lett.* **92**, 040401 (2004).
- [20] A. I. Streltsov, O. E. Alon, and L. S. Cederbaum, *Phys. Rev. Lett.* **106**, 240401 (2011).
- [21] T. Fogarty, A. Kiely, S. Campbell, and T. Busch, *Phys. Rev. A* **87**, 043630 (2013).
- [22] D. Delande, K. Sacha, M. Płodzień, S. K. Avazbaev, and J. Zakrzewski, *New J. Phys.* **15**, 045021 (2013).
- [23] B. Gertjerenken, T. P. Billam, C. L. Blackley, C. R. Le Sueur, L. Khaykovich, S. L. Cornish, and C. Weiss, *Phys. Rev. Lett.* **111**, 100406 (2013).
- [24] L. Barbiero and L. Salasnich, *Phys. Rev. A* **89**, 063605 (2014).
- [25] J. B. McGuire, *J. Math. Phys.* **5**, 622 (1964).
- [26] F. Calogero and A. Degasperis, *Phys. Rev. A* **11**, 265 (1975).
- [27] Y. Castin and C. Herzog, *C. R. Acad. Sci. Paris, Ser. IV* **2**, 419 (2001).
- [28] E. H. Lieb and W. Liniger, *Phys. Rev.* **130**, 1605 (1963).
- [29] I. E. Mazets and G. Kurizki, *Europhys. Lett.* **76**, 196 (2006).
- [30] G. E. Uhlenbeck and L. S. Ornstein, *Phys. Rev.* **36**, 823 (1930).
- [31] H. Grabert, P. Schramm, and G.-L. Ingold, *Phys. Rep.* **168**, 115 (1988).
- [32] P. Jung and P. Hänggi, *Phys. Rev. A* **44**, 8032 (1991).
- [33] G. M. Wang, E. M. Sevick, E. Mittag, D. J. Searles, and D. J. Evans, *Phys. Rev. Lett.* **89**, 050601 (2002).
- [34] B. Lukić, S. Jeney, C. Tischer, A. J. Kulik, L. Forró, and E.-L. Florin, *Phys. Rev. Lett.* **95**, 160601 (2005).
- [35] M. Köppl, P. Henseler, A. Erbe, P. Nielaba, and P. Leiderer, *Phys. Rev. Lett.* **97**, 208302 (2006).
- [36] T. Ando and J. Skolnick, *Proc. Natl. Acad. Sci. USA* **107**, 18457 (2010).
- [37] R. Steinigeweg, H.-P. Breuer, and J. Gemmer, *Phys. Rev. Lett.* **99**, 150601 (2007).
- [38] R. Metzler and J. Klafter, *Phys. Rep.* **339**, 1 (2000).
- [39] U. Siems, C. Kreuter, A. Erbe, N. Schwierz, S. Sengupta, P. Leiderer, and P. Nielaba, *Sci. Rep.* **2**, 1015 (2012).
- [40] T. Turiv, I. Lazo, A. Brodin, B. I. Lev, V. Reiffenrath, V. G. Nazarenko, and O. D. Lavrentovich, *Science* **342**, 1351 (2013).
- [41] R. Metzler and J. Klafter, *J. Phys. A: Math. Gen.* **37**, R161 (2004).
- [42] D. Dries, S. E. Pollack, J. M. Hitchcock, and R. G. Hulet, *Phys. Rev. A* **82**, 033603 (2010).
- [43] S. Sinha, A. Y. Cherny, D. Kovrizhin, and J. Brand, *Phys. Rev. Lett.* **96**, 030406 (2006).
- [44] C. Weiss and Y. Castin, *Phys. Rev. Lett.* **102**, 010403 (2009).
- [45] R. Grimm, M. Weidemüller, and Y. B. Ovchinnikov, *Adv. At. Mol. Opt. Phys.* **42**, 95 (2000).

- [46] M. H. Anderson, J. R. Ensher, M. R. Matthews, C. E. Wieman, and E. A. Cornell, *Science* **269**, 198 (1995).
- [47] M. H. A. Davis, *Markov Models and Optimization* (Chapman and Hall, London, 1993).
- [48] M. Olshanii, *Phys. Rev. Lett.* **81**, 938 (1998).
- [49] Y. Castin, *Eur. Phys. J. B* **68**, 317 (2009).
- [50] M. Bonitz, K. Balzer, and R. van Leeuwen, *Phys. Rev. B* **76**, 045341 (2007).
- [51] B. Gertjerenken, *Phys. Rev. A* **88**, 053623 (2013).
- [52] S. Flügge, *Rechenmethoden der Quantentheorie* (Springer, Berlin, 1990).
- [53] E. H. Lieb, R. Seiringer, J. P. Solovej, and J. Yngvason, in *Current Developments in Mathematics 2001* (International Press, Boston, 2002), p. 131.
- [54] B. Gertjerenken and C. Weiss, *Phys. Rev. A* **88**, 033608 (2013).
- [55] B. Gertjerenken and C. Weiss, *J. Phys. B* **45**, 165301 (2012).
- [56] A. L. Gaunt, T. F. Schmidutz, I. Gotlibovych, R. P. Smith, and Z. Hadzibabic, *Phys. Rev. Lett.* **110**, 200406 (2013).
- [57] T. F. Schmidutz, I. Gotlibovych, A. L. Gaunt, R. P. Smith, N. Navon, and Z. Hadzibabic, *Phys. Rev. Lett.* **112**, 040403 (2014).
- [58] Computer algebra program MAPLE, <http://www.maplesoft.com/>.
- [59] J. L. Helm, S. J. Rooney, C. Weiss, and S. A. Gardiner, *Phys. Rev. A* **89**, 033610 (2014).
- [60] D. I. H. Holdaway, C. Weiss, and S. A. Gardiner, *Phys. Rev. A* **85**, 053618 (2012).
- [61] Z. Shotan, O. Machtey, S. Kokkelmans, and L. Khaykovich, *Phys. Rev. Lett.* **113**, 053202 (2014).
- [62] J. Dalibard, Y. Castin, and K. Mølmer, *Phys. Rev. Lett.* **68**, 580 (1992).
- [63] R. Dum, P. Zoller, and H. Ritsch, *Phys. Rev. A* **45**, 4879 (1992).
- [64] H.-P. Breuer and F. Petruccione, *The Theory of Open Quantum Systems* (Clarendon Press, Oxford, 2006).
- [65] S. Haroche and J.-M. Raimond, *Exploring the Quantum—Atoms, Cavities and Photons* (Oxford University Press, Oxford, 2006).
- [66] A. Sinatra, C. Lobo, and Y. Castin, *J. Phys. B* **35**, 3599 (2002).
- [67] P. Bienias, K. Pawłowski, M. Gajda, and K. Rzazewski, *Europhys. Lett.* **96**, 10011 (2011).
- [68] E. H. Lieb, R. Seiringer, and J. Yngvason, *Phys. Rev. A* **61**, 043602 (2000).
- [69] G. C. Ghirardi, A. Rimini, and T. Weber, *Phys. Rev. D* **34**, 470 (1986).
- [70] W. Dür, R. Raussendorf, V. M. Kendon, and H.-J. Briegel, *Phys. Rev. A* **66**, 052319 (2002).
- [71] M. Karski, L. Förster, J.-M. Choi, A. Steffen, W. Alt, D. Meschede, and A. Widera, *Science* **325**, 174 (2009).
- [72] The data associated with this work are available at <http://dx.doi.org/10.15128/kk91fk954>.